Quantum memory based on a spatiospectral atomic comb

Mingzhen Tian, Devin Vega, and Jacob Dilles
School of Physics, Astronomy, and Computational Sciences, George Mason University Fairfax, Virginia 22030, USA
(Received 12 July 2012; revised manuscript received 19 March 2013; published 29 April 2013)

An atomic comb structure consisting of both spatial and spectral components is proposed for the implementation of quantum memory using inhomogeneously broadened atomic ensembles, such as rare-earth ions trapped in solids. The spatiospectral comb can be prepared in two-level atoms provided a third energy level is available for atomic population storage. The output photon is retrieved from the memory as a spatially diffracted photon echo. The angle between the input and output directions is controlled by the spatial component of the atomic comb. The memory efficiency is analyzed using coupled wave theory, which results in memory efficiency varying with the retrieval angle: 54.1% in collinear, 81.6% in perpendicular, and 100% in counterpropagating configurations. An experimental method for creating a multidimensional atomic comb is suggested.

DOI: 10.1103/PhysRevA.87.042338 PACS number(s): 03.67.Hk, 42.50.Md, 42.50.Gy, 42.40.Pa

I. INTRODUCTION

In recent years, the atomic frequency comb (AFC) has rapidly emerged as an important approach for implementation of a practical quantum memory [1,2]. AFCs made of rare-earth ensembles trapped in inorganic crystals are distinguished by the combination of superior performance metrics including high efficiency up to 100%; long on-demand storage time, up to seconds; and scalable multiple-mode operation with a high time-bandwidth product, up to 10^5. Investigation of the AFC has gained exceptional momentum since the first protocol originally proposed in 2008 [3]. Separate experimental demonstrations highlight progresses in memory efficiency up to 35% for a single mode bright pulse [4], 1060 temporal mode storage with gigabit per second bit rate [5], storage of entangled photonic states [6,7], and recently, storage of photon-polarization states [8]. One of the most critical metrics to enable AFC quantum memory is memory efficiency. Prior experimental results are below the 50% efficiency, the threshold required for the quantum no-cloning regime [9]. While theoretical analysis has concluded that achieving up to 54% efficiency for forward retrieval is possible [10,11], considering the effects of atomic decoherence and experimental error, it is unlikely that 50% efficiency will be realized with a forward retrieval scheme.

A backward retrieval is more promising, as theoretical analysis shows a potential for 100% efficiency [10,11]. However, the existing backward retrieval scheme requires a three-level system and two extra counterpropagating control pulses to transfer the quantum state between optical and spin coherences during the storage and retrieval stages [3]. This makes the processes of AFC preparation, storage, and retrieval difficult to implement and complicated to control. No experimental demonstration for backward retrieval has been performed to date. An AFC memory with spin-wave storage and forward retrieval has been reported [12], which demonstrated the effect of optical-spin coherence transfer by a control pulse pair applied in the backward direction with respect to the input and retrieved signals. The low memory efficiency (2.8%) in the experiment was attributed mainly to the inhomogeneous spin dephasing and the imperfect spatial mode overlap between the counterpropagating input and control pulse pair.

To overcome these obstacles, we propose using an atomic comb structure in both frequency and space: a spatiospectral atomic comb (S2AC). This scheme offers more flexibility in a relatively simple physical system, allowing backward retrieval in a two-level system and eliminating the need for a control pulse pair. The S2AC forces the retrieved signal to propagate in a direction that obeys the Bragg condition for a spatially thick volume hologram [13]. The angle between the input and output beams may be set arbitrarily by manipulating the spatial components of the atomic comb. The theoretical upper limit for the memory efficiency varies from 54.1% in the collinear case to 100% in the counterpropagating case. Compared with the existing schemes, S2AC offers more flexibility in a relatively simple physical system for setting up a quantum memory. It may lead to experimental demonstration of memory efficiency above the 50% threshold.

II. BACKWARD RETRIEVAL IN A TWO-LEVEL SYSTEM

An S2AC is made of an ensemble of two-level atoms in the ground state with their optical resonant frequencies arranged into a periodic comb shape in both frequency and space. Figure 1 illustrates the ground-state population of an S2AC that will result in backward retrieval with the temporal and spatial configuration and the relevant energy levels shown in Fig. 2. In the S2AC, the atomic comb structure is featured with identical sharp spikes periodically distributed with frequency spacing Γ and spatial period $\lambda/2$ in the z direction. When an input photon incident along the z direction is absorbed by an S2AC consisting of N atoms, the photon is stored as the collective optical excitation of the atoms as $|\psi_0\rangle = \sum_{j=1}^{N} e^{ikz_j}|g_1\cdots e_j\cdots g_N\rangle/\sqrt{N}$, where $|g_j\rangle$ and $|e_j\rangle$ represent the ground and excited states for the jth atom at location z_j; $k = 2\pi/\lambda$ is the photon's propagation constant. For simplicity, it is assumed that all atoms share the same transition probability. After time t, due to the inhomogeneous detuning of the atomic resonance, the atomic coherence dephases to

$$|\psi(t)\rangle = \sum_{j=1}^{N} e^{i2\pi\delta_j t + ikz_j}|g_1\cdots e_j\cdots g_N\rangle/\sqrt{N}, \qquad (1)$$

where δ_j denotes the frequency detuning for the jth atom. In an S2AC, the frequency detuning of an atom at z_j is preprogrammed to satisfy $\delta_j = n_j\Gamma - 2\Gamma z_j/\lambda$. At time

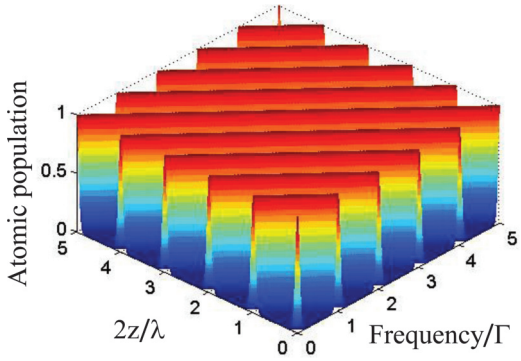

FIG. 1. (Color online) S2AC represented by the normalized ground-state population as a function of frequency and space. Γ and $\lambda/2$ are the periods in frequency and space, respectively.

$t = 1/\Gamma$, the optical coherence in Eq. (1) rephases as

$$|\psi(t = 1/\Gamma)\rangle = \sum_{j=1}^{N} e^{-ikz_j}|g_1 \cdots e_j \cdots g_N\rangle/\sqrt{N}. \quad (2)$$

As a result of constructive interference of the atomic coherence, the retrieved signal from the memory (of storage time $1/\Gamma$) is a photon echo emitted in a direction ($-z$ direction) opposite to the input. Figures 2(a) and 2(b) illustrate the timing and the direction for the input and output photons in the storage and retrieval process. In this scheme, the backward retrieval is achieved in a two-level system without the help of the control pulse pair and optical-spin coherence conversion. The counterpropagation of the retrieved photon is accomplished by the spatial component of the S2AC in a similar way as a spatial volume hologram. As an inherent feature for backward retrieval, the memory efficiency in this scheme has a theoretical upper limit of 100%, which will be derived in the next section.

III. MEMORY EFFICIENCY

Various spatial configurations for counterpropagation and angled-beam settings are well known in simulated photon-echo processes where spatiospectral gratings result in output photon-echo signals both temporally delayed and spatially diffracted [14–16]. The spatial part of the grating works the same way as Bragg diffraction in a thick hologram except for the spatial asymmetry caused by causality [14]. The temporal and spatial characteristics of the storage and retrieval of a photon in an S2AC are similar to a stimulated photon-echo process, with two differences critical for quantum memory.

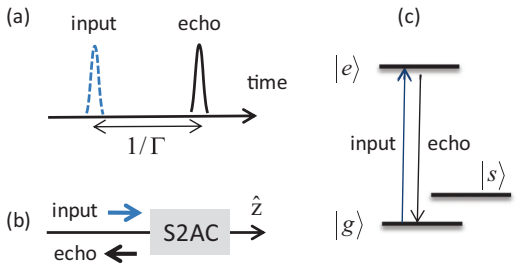

FIG. 2. (Color online) (a) Temporal, and (b) spatial configurations of a backward retrieval process in an S2AC. (c) Relevant energy levels.

First, an S2AC consists of ground-state atoms only, while the spatiospectral grating that produces a regular stimulated photon echo is made of an atomic population in both ground and excited states. Suppression of spontaneous emission by eliminating the excited-state population is mandatory for achieving high fidelity in a quantum memory. Second, the S2AC is a periodic comb structure with sharp spikes much narrower than the period, whereas the grating for a stimulated photon echo resembles a sinusoidal function in both space and frequency. A larger ratio between the period and the linewidth of a comb spike, usually defined as finesse in the AFC and S2AC, is required to maximize memory efficiency. These differences in the atomic population distribution in space and frequency are made in the stage of programming a medium, a process that usually begins with all atoms initially in the ground state. Both structures can be created in similar processes through optical excitation with different parameter settings. In fact, an optical pumping scheme involving the repetitive excitation and relaxation, which is used in the accumulated stimulated photon-echo process has also been used in programming AFCs in a collinear configuration. In this case, the programming pulse pairs and the input and output propagate in the same direction [3,11,17].

This process can be adapted to an angled-beam configuration where the two pulses in a programming pair propagate along two directions with an angle θ as shown in Fig. 3(a). The spectral component of the grating stays the same, while the spatial component is characterized by a grating vector $\vec{K}$. The wave vectors for the input ($\vec{k}_s$) and output ($\vec{k}_1$) photons should satisfy the Bragg condition: $\vec{k}_1 = \vec{k}_s + \vec{K}$. Without

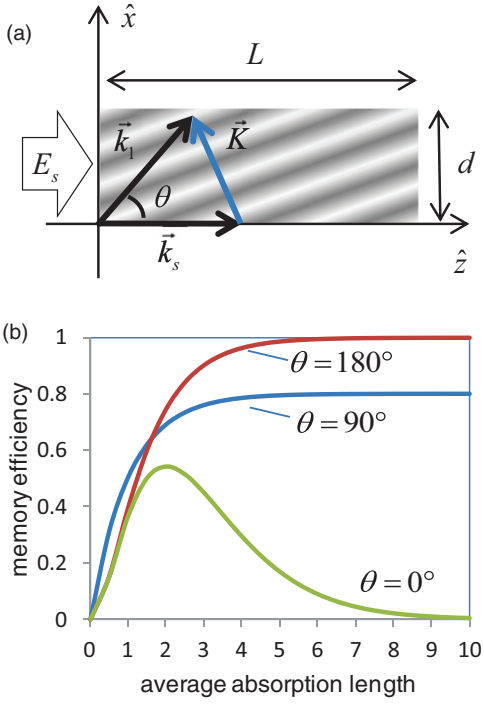

FIG. 3. (Color online) (a). Spatial grating and diffraction in L-long and d-wide medium. $\vec{k}_s$, $\vec{k}_1$, and $\vec{K}$ denote the wave vectors of the input, output, and the spatial grating. E_s represents the input field. (b). Maximum memory efficiency vs average absorption length in the z direction for collinear, perpendicular, and backward configurations.

losing generality, we assign the first programming pulse along the z direction and the second along a direction in the z-x plane and with angle θ from the z axis. The grating vector $\vec{K} = 2k \sin\frac{\theta}{2}(\cos\frac{\theta}{2}\hat{x} - \sin\frac{\theta}{2}\hat{z})$ as shown in Fig. 3(a) is defined in the z-x plane. Wave vectors $\vec{k}_1$ and $\vec{k}_s$ should have the same magnitude of k. After an atomic comb is prepared, the storage and retrieval involve either single photon or weak coherent light propagating through a periodic medium. For the purpose of calculating the memory efficiency, the process of storage and retrieval is linear and can be analyzed with full quantum [18], semiclassical [10], or classical models [11]. We will use a classical coupled wave theory to study the memory efficiency in an S2AC, which was originally developed for the volume hologram and later applied to accumulated simulated photon echoes [14,15,19].

A scalar electric field representing a weak laser pulse or a photon wave packet is defined as

$$\mathbf{E}(t,\vec{R}) = E(t,\vec{R})e^{-i2\pi\nu_0 t} + \text{c.c.}, \tag{3}$$

where ν_0 is the center frequency of the pulse and $\vec{R} = x\hat{x} + z\hat{z}$ denotes a location in the medium in the z-x plane. The medium and the field are assumed uniform in the y direction. The complex time-domain function $E(t,\vec{R})$ is related to the field $\tilde{E}(\nu,\vec{R})$ in the frequency domain through a Fourier transform as $E(t,\vec{R}) = \int \tilde{E}(\nu,\vec{R})e^{-i2\pi t}d\nu$. The field in the frequency domain satisfies the wave equation as

$$\nabla^2\tilde{E}(\nu,\vec{R}) + k^2\varepsilon_r(\nu,\vec{R})\tilde{E}(\nu,\vec{R}) = 0. \tag{4}$$

The relative permittivity $\varepsilon_r(\nu,\vec{R})$ carries the spatiospectral comb, which is directly determined by the absorption coefficient $\alpha(\nu,\vec{R})$ through the Kramers-Kronig relation as

$$\varepsilon_r(\nu,\vec{R}) = 1 - ik^{-1}(1 + i\hat{\mathcal{H}})\alpha(\nu,\vec{R}), \tag{5}$$

where the Hilbert operator is defined as

$$\hat{\mathcal{H}}\alpha(\nu,\vec{R}) = \frac{1}{\pi}\int \frac{\alpha(\nu',\vec{R})}{\nu' - \nu}d\nu'. \tag{6}$$

In an S2AC, the absorption coefficient that is proportional to the ground-state population can be expressed as a normalized narrow spectral function $\xi(\nu)$ convolved with a spatiospectral Dirac delta comb $D(\nu,\vec{R})$ as

$$\alpha(\nu,\vec{R}) = \alpha_0\xi(\nu) \otimes D(\nu,\vec{R}), \tag{7}$$

where α_0 is the peak absorption coefficient and is assumed constant. The Dirac delta comb in space and frequency is defined as

$$D(\nu,\vec{R}) = \sum_{n=-\infty}^{\infty}\delta\left(\nu - \left(n + \frac{\vec{K}\cdot\vec{R}}{2\pi}\right)\Gamma\right), \tag{8}$$

which is a periodic function both in spectrum with a period of Γ and in space with a period of $\lambda/(2\sin\frac{\theta}{2})$ along the direction of $\vec{K}$.

The periodic absorption coefficient can be expanded into a Fourier series as

$$\alpha(\nu,\vec{R}) = \alpha_0\sum_{m=-\infty}^{\infty}A_m e^{im2\pi\tau - im\vec{K}\cdot\vec{R}},$$

with $\tau = 1/\Gamma$. The Fourier components for an S2AC defined in Eqs. (7) and (8) are calculated as

$$\begin{aligned} A_m &= \frac{1}{(2\pi)^2}\int \alpha(\nu,\vec{R})e^{-im2\pi\tau + im\vec{K}\cdot\vec{R}}d\nu d\vec{R} \\ &= \frac{1}{\Gamma}\int \xi(\nu)e^{-im2\pi\tau}d\nu. \end{aligned} \tag{9}$$

Similarly, the field can be written into multiple spatiotemporal modes as

$$\tilde{E}(\nu,x,z) = \sum_{p=-\infty}^{\infty}E_p e^{ip2\pi\tau - ip\vec{K}\cdot\vec{R} - ikz}. \tag{10}$$

The zero-order ($p = 0$) field peaks at $t = 0$ and propagates in the z direction with wave vector $k\hat{z}$. The first-order ($p = 1$) field occurs around $t = 1/\Gamma$ and propagates with wave vector $k\hat{z} + \vec{K}$. Higher-order modes only exist under the condition of a small angle that satisfies, $p(p-1)L\theta^2/\lambda \ll 1$, where L is the medium length along the z direction. Since the medium length is usually many orders of magnitude greater than the wavelength, this condition is practically satisfied only at $\theta = 0$ for any orders higher than 1.

According to Eqs. (4)–(8), the zero- and first-order fields should obey

$$\frac{\partial}{\partial z}E_0 + \frac{\alpha_0 A_0}{2}E_0 = 0, \tag{11}$$

$$\begin{aligned} &\frac{k + K_z}{k}\frac{\partial}{\partial z}E_1(x,z) + \frac{K_x}{k}\frac{\partial}{\partial x}E_1(x,z) + \frac{\alpha_0 A_0}{2}E_1(x,z) \\ &\quad + \alpha_0 A_1 E_0(z) = 0, \end{aligned} \tag{12}$$

where the second-order derivatives are ignored by applying the slow-varying envelope approximation. Equation (11) governs the propagation of the input field in the z direction. The field amplitude E_0 is a function of z and keeps the same temporal shape as the input. The first-order field in Eq. (12) represents the diffraction from the S2AC. Since it propagates in the direction of $k\hat{z} + \vec{K}$ the field amplitude is both z and x dependent in general, as shown in the first two terms of Eq. (12). The third term in the equation represents the absorption of the diffracted field through the medium. The last term takes into account the coupling from the zero order to the first order, which is the source of the output signal. These characteristics are all similar to a thick spatial hologram. However, two significant differences between the S2AC diffraction and thick spatial hologram are worth noting: First, the diffracted field is temporally delayed by $\tau = 1/\Gamma$ with respect to the input field and, second, the first-order echo field does not couple back to the zero-order field due to causality-related asymmetry [14,19] for diffraction in S2AC, which is mathematically embedded in the Hilbert transform in Eq. (5).

Due to the lack of feedback from the echo, the input field equation can be readily solved as

$$E_0(z) = E_s e^{-\bar{\alpha}z/2}, \tag{13}$$

where E_s denotes the input field amplitude, and $\bar{\alpha} = \alpha_0 A_0 = \alpha_0\int\xi(\nu)d\nu/\Gamma$ is the intensity absorption coefficient averaged over a spectral period. According to Eq. (13), the input field

propagates through an S2AC with an exponentially decreasing amplitude due to the absorption at an average coefficient, $\bar{\alpha}/2$.

According to Eqs. (12) and (13), three important cases, $\theta = 0^\circ, 90^\circ, 180^\circ$, can be solved analytically with well-defined spatial boundary conditions in an S2AC. They correspond, respectively, to forward, perpendicular, and backward propagations for the echo field with respect to the input.

In the case of forward propagation, $\vec{K} = 0$, the atomic comb becomes one dimensional in frequency and independent of space. Equation (12) is simplified into

$$\frac{\partial}{\partial z}E_1(z) + \frac{\alpha_0 A_0}{2}E_1(z) + \alpha_0 A_1 E_s e^{-\bar{\alpha}z/2} = 0.$$

The first-order echo amplitude for a medium length L in the z direction can be solved as

$$E_1 = -\bar{\alpha}L\frac{A_1}{A_0}E_s e^{-\bar{\alpha}L/2}.$$

The memory efficiency is calculated as

$$\eta = \left|\frac{E_1}{E_s}\right| = \left(\frac{A_1}{A_0}\right)^2 (\bar{\alpha}L)^2 e^{-\bar{\alpha}L},$$

which maximizes at $\eta \sim 54.1\%$ under the conditions $\bar{\alpha}L = 2$ and $A_1/A_0 \sim 1$. This is consistent with the results for the AFC [10,11].

In the case of backward propagation, the echo field propagates in the $-z$ direction under the condition $\theta = 180^\circ$ with a spatial grating vector specified as $\vec{K} = -2k\hat{z}$. The characteristic Dirac comb becomes two dimensional as $D(\nu,z) = \sum_{n=-\infty}^{\infty}\delta(\nu - (n - 2z/\lambda)\Gamma)$. The echo field amplitude is independent of x and Eq. (12) becomes

$$\frac{\partial}{\partial z}E_1(z) - \frac{\alpha_0 A_0}{2}E_1(z) - \alpha_0 A_1 E_s e^{-\bar{\alpha}z/2} = 0. \quad (14)$$

Equation (14) can be solved as $E_1 = -\frac{A_1}{A_0}E_s(1 - e^{-\bar{\alpha}L})$ with the corresponding memory efficiency,

$$\eta = \left(\frac{A_1}{A_0}\right)^2 (1 - e^{-\bar{\alpha}L})^2. \quad (15)$$

This is exactly the same result as for one-dimensional AFC in the backward retrieval scheme [10,11], although the mechanisms that cause backward propagation in AFC and S2AC are completely different. A_1/A_0 denotes the ratio between the temporal responses of the spectral spike in the atomic comb at $t = 0$ and $1/\Gamma$. Theoretically, the proper selection of average absorption length, finesse, and spike shape can set $e^{-\bar{\alpha}L} \to 0$ and $A_1/A_0 \to 1$. Under such conditions and neglecting decoherence in the atomic ensemble, the memory efficiency approaches the theoretical upper limit of 100%.

In an S2AC programmed for $\theta = 90^\circ$, i.e., $\vec{K} = k\hat{x} - k\hat{z}$, the echo field propagates in the perpendicular direction with respect to the input. The Dirac delta comb takes the shape $D(\nu,\vec{K}\cdot\vec{R}) = \sum_{n=-\infty}^{\infty}\delta(\nu - (n + x/\lambda - z/\lambda)\Gamma)$. The first term in Eq. (12) is eliminated and the equation can be rewritten as

$$\frac{\partial}{\partial x}E_1(x,z) + \frac{\alpha_0 A_0}{2}E_1(x,z) + \alpha_0 A_1 E_s e^{-\bar{\alpha}z/2} = 0. \quad (16)$$

The second term in Eq. (16) represents the absorption for an echo field that propagates in the x direction. The third term indicates that, for any location (x, z) in the volume of the input beam path, the S2AC turns the local input field to a source that generates the echo field propagating in the perpendicular direction. Solving this equation for the echo field at the output side of the medium $x = d$,

$$E_1(d,z) = 2\frac{A_1}{A_0}E_s(e^{-\bar{\alpha}d/2} - 1)e^{-\bar{\alpha}z/2}.$$

In this configuration, the spatial cross sections of the input and output beams are of different sizes. The ratio of the power, rather than intensity, must be calculated. The resulting memory efficiency depends on the absorption lengths in both z and x directions as

$$\eta = 4\left(\frac{A_1}{A_0}\right)^2 \frac{(e^{-\bar{\alpha}d/2} - 1)^2}{\bar{\alpha}d}(1 - e^{-\bar{\alpha}L}). \quad (17)$$

The memory efficiency should be optimized for both absorption lengths. Efficiency maximizes at ~81.6% under the conditions $\bar{\alpha}L \to \infty$, $\bar{\alpha}d \approx 2.5$, and $A_1/A_0 \to 1$.

Memory efficiencies for backward, perpendicular, and forward configurations are plotted in Fig. 3(b). At any given $\bar{\alpha}L$, the condition is assumed optimal for $A_1/A_0 \to 1$ in all cases and $\bar{\alpha}d \approx 2.5$ for perpendicular setting. The plot shows at relatively low absorption length $\bar{\alpha}L < 1.6$ that the perpendicular echo has the highest efficiency among the three cases, up to ~63.7%. Beyond this point, the backward configuration has the highest efficiency, up to 100% at large $\bar{\alpha}L$. The perpendicular echo has a similar dependence on the average absorption length with a lower maximum efficiency at ~81.6%. The forward configuration shows a quite different curve with efficiency maximizing at ~54.1% for $\bar{\alpha}L = 2$, declining at larger absorption length. It is clear high efficiency favors the spatial configurations for backward and perpendicular echoes. It would be reasonable to expect the maximum efficiency will not be greatly affected if the orientation of the spatial grating is slightly shifted in all three cases due to misalignment in the programming stage. This provides more options and tolerance in angled-beam setups for high efficiency memory.

IV. CONSIDERATIONS ON PROGRAMMING S2ACs

The process of making an atomic comb is similar to creating a spectral or spatiospectral grating in an accumulated stimulated photon-echo process. In both cases, the comb and grating are formed in the difference of the atomic populations in the ground and the excited states. However, the latter usually consists of contributions from both states while the former has to be strictly from the ground state only while the excited state must be empty. An S2AC can be created through repetitive optical pumping combined with atomic population decay. According to a given frequency spacing Γ, the atomic population that is initially in the ground state at all frequencies and spatial locations is cycled through all three energy levels as shown in Fig. 2(c) and eventually redistributed among the ground and population shelving levels. At the end of the process, the atoms in the ground state make up the desired spatiospectral comb structure. The excited state is empty with all unwanted atoms moved to a long-life population shelving level.

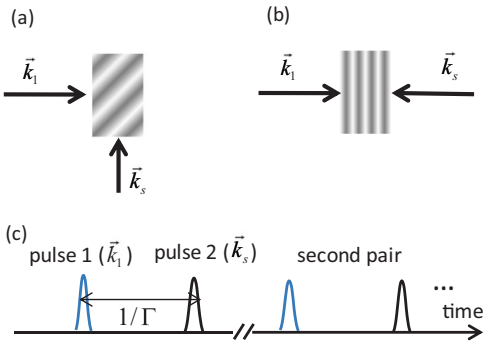

FIG. 4. (Color online) Spatial grating for perpendicular (a) and backward (b) configurations. (c). The temporal configuration of the pumping pulses in preparation of an S2AC. $\vec{k}_s$ and $\vec{k}_1$ denote the wave vectors of the first and second pulses, respectively, in a pumping pulse pair.

Unlike the one-dimensional frequency comb where the programming is performed with repetitive pulse pairs in one beam, programming an S2AC requires pulses in two beams as illustrated in Figs. 4(a) and 4(b). In order to create an S2AC according to the Dirac delta comb $D(\nu,z) = \sum_{n=-\infty}^{\infty} \delta(\nu - (n - 2z/\lambda)\Gamma)$ shown in Fig. 1 for backward retrieval, the first (second) pulse in a pulse pair should come in along z ($-z$) direction with a time delay of $\tau = 1/\Gamma$. The pulse pair forms an interference pattern in space and frequency proportional to a sinusoidal function with crests at $\nu - (n + 1/2 - 2z/\lambda)\Gamma$ and troughs at $\nu - (n - 2z/\lambda)\Gamma$ for integer number n. When a single shot of such a pulse pair is set weak enough to keep the excitation in the linear regime, the atomic population inversion takes the imprint of the interference pattern. When multiple subsequent shots are applied, the atomic population inversion deviates from the sinusoidal shape due to saturation around the crests. The result is a much broader spectrum of excited atoms around the crests than that of the atoms unexcited around the troughs. In the population decay following each pumping pulse pair, part of the excited-state atomic population relaxes to the shelving state instead of returning to the ground state. A proper combination of the pulse pair, repetition time, and total pumping length should result in the desired final atomic population in the ground state, an empty excited state, and a shelving state holding the rest of the atoms. This process should produce an ideal S2AC under the conditions that the medium is optically thin, the spatial modes of the counterpropagating beams match in the medium, and the relative phase between the two pulses are stable during the accumulation. Among the three conditions, only the last one is evident in existing experiments, such as in references [19,20]. The other two need further discussion since an S2AC needs a highly absorptive medium to achieve high memory efficiency, and spatial mode matching of counterpropagating beams has to be shown an experimental challenge in AFC [12].

Accumulated pumping has been demonstrated in programming AFCs in optically thick medium. However, the method may not apply to the preparation of an S2AC directly with two counterpropagating pulses. Due to strong absorption, neither of the two pulses may propagate long enough to build a significant contrast in the interference pattern throughout the medium. In order to ameliorate this problem, one can start from a medium with a half-inverted population, which can be achieved in a thick medium with good uniformity in space and spectrum [21]. Since the absorption coefficient in a medium is proportional to the population difference between the ground and excited states, the initial absorption vanishes without the population difference and a thick medium becomes optically transparent. The first programming shot is delayed for a short time to allow a small portion of the population to decay from the excited state back to the ground state. Then, the population in the ground state is slightly higher than the excited state and the absorption is weak, but nonzero. With an initially weak absorption, the counterpropagating programming pulses keep the field amplitude nearly constant throughout the medium, which results in high contrast in the interference pattern. Repeating the pattern for a large number of shots while the excited population gradually decays to the ground and shelving states builds up an S2AC with the spatial comb along the z direction in an optically thick medium. A similar scheme can be used to prepare an S2AC for a perpendicular configuration as shown in Fig. 4(a). As the atomic population is shaped into an S2AC, the average absorption is expected to increase, which may make the programming field amplitudes off balance at both ends of the medium. Contrast of the interference will become higher in the middle of the medium and lower at both ends. As a result, the S2AC will be less ideal at the ends than the middle. This effect requires further investigation, most likely with numerical simulations based on the Maxwell-Bloch equations [16].

The purpose of spatial mode matching of the counterpropagating beams in both AFC and S2AC is for the input photon wave packet to interact with a high contrast and spatially uniform atomic comb. This usually requires that the spatial modes match for all beams including the programming, input signal, and control beams. S2AC uses a counterpropagating beam in the programming stage rather than the storage and retrieval stage as in AFC. This makes the spatial mode matching in S2AC easier than the control π-pulse pair in AFC. The main reasons are that the programming pulses are relatively weak, much less than a π pulse, and the frequency is the same as the input and retrieved signals. Since the Rabi frequency is inversely proportional to the beam diameter, the programming beams do not need to focus as tightly as the control beams. The spatial mode matching between the programming pulses is easier to adjust. All pulses involved in programming and storage can be generated through electronically controlled acousto-optical modulators. The counterpropagating beam paths can be made symmetric in the medium since no physical path length difference is required. This will help to match the spatial modes. Moreover, the spatial mode of the input signal automatically matches with one of the programming pulses since they have the same frequency and beam path. On the other hand, the frequency shift between the input and control pulses in AFC makes the spatial modes more difficult to match. It is worth noting a possible setting to meet the assumption of both optically thin medium and good spatial mode matching in a low finesse cavity where thin media with low absorption in single path can be used to achieve effectively high absorption and memory efficiency [22].

Compared with the AFC in three-level atomic ensembles, the S2AC is designed for two-level systems. While the S2AC may favor high efficiency with a relatively simple setup, other memory properties should be evaluated with reference to the AFC. In two-level systems where no optical-spin transfer is involved, the storage time is the time for rephasing of the coherence, which is also the delay time between the input and its echo. This is preprogrammed in the frequency spacing in the S2AC, no longer adjustable in the retrieval process. The retrieval is no longer on demand. The upper limit for the storage time is the optical coherence time, which is usually shorter than the spin coherence, but can still be considerably long, on the millisecond scale for some materials [23]. Memory capacity for multiple temporal modes in the S2AC is not affected compared with the AFC since the optical dephasing and rephasing process stays the same in both structures.

V. CONCLUSION

A quantum memory protocol is proposed for two-level atomic ensembles to achieve memory efficiency higher than 50%, the threshold for the quantum no-cloning regime. An S2AC, as a comb structure in both frequency and space, is analyzed as memory for a single photon or weak coherent pulse. The retrieved signal is both temporally delayed and spatially diffracted, and can propagate in any spatial direction programmed in the spatial comb of the S2AC. The storage and retrieval process is analyzed using coupled wave theory. The upper limit of memory efficiency varies with retrieval angle, from 54.1% in collinear, to 81.6% in perpendicular, to 100% in counterpropagating configurations. This approach offers more flexibility for implementing a quantum memory. A possible experimental arrangement is considered for creating an S2AC in an optically thick medium while a further numerical procedure is needed for more accurate evaluation.

ACKNOWLEDGMENTS

Authors would like to acknowledge Professor Karen Sauer at George Mason University for helpful discussions. This work was supported by a grant from Office of Naval Research (Grant No. 09PR08570-00/1054998) and National Science Foundation (Grant No. PHY-1212360).

[1] C. Simon, M. Afzilius, J. Appel, A. B. de la Giroday, S. J. Dewhurst, N. Gisin, C. Hu, F. Jelezko, S. Kröll, J. H. Müller, J. Nunn, E. Polzik, J. Rarity, H. de Riedmatten, W. Rosenfeld, A. J. Shields, N. Sköld, R. M. Stevenson, R. Thew, I. Walmsley, M. Weber, H. Wienfurter, J. Wrachtrup, and R. J. Young, Eur. Phys. J. D **58**, 1 (2010).

[2] W. Tittel, M. Afzilius, T. Chanelière, R. L. Cone, S. Kröll, S. A. Moiseev, and M. Sellars, Laser Photonics Rev. **4**, 244 (2009).

[3] H. de Riedmatten, M. Afzelius, M. U. Staudt, C. Simon, and N. Gisin, Nature **456**, 773 (2008).

[4] A. Amari, A. Walther, M. Sabooni, M. Huang, S. Kröll, M. Afzilius, I. Usmani, B. Lauritzen, N. Sangouard, H. de Riedmatten, and N. Gisin, J. Lumin. **130**, 1579 (2010).

[5] M. Bonarota, J.-L. Le Gouet, and T. Chaneliere, New J. Phys. **13**, 013013 (2011).

[6] C. Clausen, I. Usmani, F. Bussières, N. Sangouard, M. Afzilius, H. de Riedmatten, and N. Gisin, Nature **469**, 508 (2011).

[7] E. Saglamyurek, N. Sinclair, J. Jin, J. A. Slater, D. Oblak, F. Bussières, M. George, R. Ricken, W. Sohler, and W. Tittel, Nature **469**, 512 (2011).

[8] C. Clausen, F. Bussières, M. Afzelius, and N. Gisin, Phys. Rev. Lett. **108**, 190503 (2012); M. Gündoğan, P. M. Ledingham, A. Almasi, M. Cristiani, and H. de Riedmatten, *ibid.* **108**, 190504 (2012); Z.-Q. Zhou, W.-B. Lin, M. Yang, C.-F. Li, and G.-C. Guo, *ibid.* **108**, 190505 (2012).

[9] M. P. Hedges, J. J. Longdell, Y. Li, and M. Sellars, Nature **465**, 1052 (2010).

[10] M. Afzelius, C. Simon, H. de Riedmatten, and N. Gisin, Phys. Rev. A **79**, 052329 (2009).

[11] T. Chanelière, J. Ruggiero, M. Bonarota, M. Afzelius, and J.-L. Le Gouët, New J. Phys. **12**, 023025 (2010).

[12] M. Afzelius, I. Usmani, A. Amari, B. Lauritzen, A. Walther, C. Simon, N. Sangouard, J. Minár, H. de Riedmatten, N. Gisin, and S. Kröll, Phys. Rev. Lett. **104**, 040503 (2010).

[13] H. Kogelnik, Bell Syst. Tech. J. **48**, 2909 (1969).

[14] A. Renn, U. P. Wild, and A. Rebane, J. Phys. Chem. **106**, 3056 (2002).

[15] H. Sõnajalg and P. Saari, J. Opt. Soc. Am. **11**, 372 (1994).

[16] T. Chang, M. Tian, and W. R. Babbitt, J. Lumin. **108**, 138 (2004).

[17] M. Bonarota, J. Ruggiero, J.-L. Le Gouët, and T. Chanelière, Phys. Rev. A **81**, 033803 (2010).

[18] S. A. Moiseev and S. Kröll, Phys. Rev. Lett. **87**, 173601 (2001).

[19] M. Tian, J. Zhang, I. Lorgeré, J.-P. Galaup, and J.-L. Le Gouët, J. Opt. Soc. Am. B **15**, 2216 (1998).

[20] M. Tian, J. Zhao, Z. Cole, R. Reibel, and W. R. Babbitt, J. Opt. Soc. Am. B **18**, 673 (2001).

[21] Zaharullah, M. Tian, T. Chang, and W. R. Babbitt, J. Lumin. **127**, 158 (2007).

[22] M. Afzelius and C. Simon, Phys. Rev. A **82**, 022310 (2010).

[23] R. M. Macfarlane and R. M. Shelby, in *Spectroscopy of Crystals Containing Rare Earth Ions*, edited by A. A. Kaplyanskii and R. M. Macfarlane (Elsevier Science Publishers, Amsterdam, 1987), Chap. 3, p. 51.